AIP | Journal of Applied Physics

Liquid separation by a graphene membrane

E. E. Fileti, G. M. Dalpian, and R. Rivelino

Citation: J. Appl. Phys. **108**, 113527 (2010); doi: 10.1063/1.3518507
View online: http://dx.doi.org/10.1063/1.3518507
View Table of Contents: http://jap.aip.org/resource/1/JAPIAU/v108/i11
Published by the AIP Publishing LLC.

Liquid separation by a graphene membrane

E. E. Fileti,[1,a)] G. M. Dalpian,[1,b)] and R. Rivelino[2,c)]
[1]*Centro de Ciências Naturais e Humanas, Universidade Federal do ABC, 09210-270 Santo André-SP, Brazil*
[2]*Instituto de Física, Universidade Federal da Bahia, 40210-340 Salvador-BA, Brazil*

(Received 12 August 2010; accepted 23 October 2010; published online 10 December 2010)

The behavior of liquids separated by a single graphene membrane has been studied with extensive molecular dynamics (MD) simulations at ambient conditions. With the help of appropriate empirical potentials, we have exploited two liquid phases forming distinct systems; say XGY, where G stands for graphene and X (Y) represents water (W), benzene (B), or acetonitrile (A). Our MD simulations revealed important changes in the wettability patterns of these liquids near the graphene surface. For instance, WGW exhibits strong density oscillations in a thin interfacial region with thickness of ~2.4 nm. In the case of BGB and AGA the oscillating-density interfacial region extends beyond ~3 nm and ~5 nm, respectively, under ambient conditions. More interestingly, our findings indicate that a liquid at one side of the graphene sheet can affect the degree of wetting on the other side, by means of dispersion interactions through the graphene membrane. These systems can offer a useful framework to understand the structural as well as thermodynamic properties of interfaces by considering a real two-dimensional substrate. © *2010 American Institute of Physics*.
[doi:10.1063/1.3518507]

I. INTRODUCTION

Graphene membranes with macroscopic size have recently been fabricated and found to be firm and difficult to bend.[1] In this sense, samples of these two-dimensional carbon films are thought to be used in much different experimental arrangements.[2] Because of the unexpected stiffness of graphene crystals, Booth *et al.*[1] have proposed that a monolayer can be used as an ideal support for atomically resolved experiments. Also, as demonstrated by Bunch *et al.*,[3] a graphene sheet is impermeable to gases, including helium, and can support pressure differences higher than 1 atm (see for example MD simulations in Ref. 4). On this basis, we idealize a device where a monolayer graphene membrane could be used to separate two distinct liquid media. This corresponds to the thinnest possible membrane that is composed of a single layer of atoms. Due to its reduced thickness, it should present properties that are not observed in normal membranes, but that should be taken into account when using it for this purpose. Recent reports have also shown unusual effects when a graphene membrane is exposed to different mediums in each of its sides.[5]

We present results from extensive molecular dynamics (MD) simulations, revealing the frontier behavior for different liquids separated by this two-dimensional (2D) membrane. Regarding both the chemical and mechanical stability of graphene, future experiments will allow a microscopic understanding of the structures of liquids near graphene interfaces.[6,7] The microscopic description of liquids separated by a membrane is of great interest in physical, chemical, and biological sciences. The main problem is saying how the molecules of the separated medium interact with the constituents of the membrane and how the molecules can induce interactions in the liquid molecules on the other side of the membrane. This characterizes an interesting interface problem,[8] since it involves a triphasic medium (XGY), where X represents the liquid at one side of graphene (G) and Y the liquid at the other side. In these systems there might be interactions between X and G, G and Y, and also between X and Y, since graphene is a one atom thick membrane. For instance, recent first-principles calculations[9] have demonstrated that water adsorbates on graphene can change the electronic properties of a SiO_2 substrate. Thus, to better understand this kind of systems we need experiments seeing in a scale of "few" atoms and theories properly treating a large-scale many-particle problem. A useful characterization of solvated membranes is often done by using phenomenological concepts of hydrophobic and hydrophilic walls.[10,11] Theoretically, this problem has successfully been treated by performing computer simulation studies.[12–14]

Diverse theoretical studies on liquid structuring and ion binding at the interfaces with polar and nonpolar walls have been carried out by using classical MD simulations.[14–25] In this line, the interfacial behavior of polyelectrolyte backbones in contact with graphene substrates has been examined.[26,27] A more detailed understanding of the interaction between a liquid phase and graphene was recently given via *ab initio* MD (AIMD) simulations.[28] This study revealed strong water density oscillations, typical of liquids near a hard wall. More interesting, the structural properties of interfacial water between graphene sheets calculated with AIMD simulations have been shown to give similar patterns to those obtained with classical MD simulations, depending on a suitable choice of intermolecular potential models.[28] Despite the success of classical MD simulations in describing a water-graphene interface, the structure of different liquids separated by a single graphene membrane has not yet been inves-

[a)]Electronic mail: fileti@ufabc.edu.br.
[b)]Electronic mail: gustavo.dalpian@ufabc.edu.br.
[c)]Electronic mail: rivelino@ufba.br.

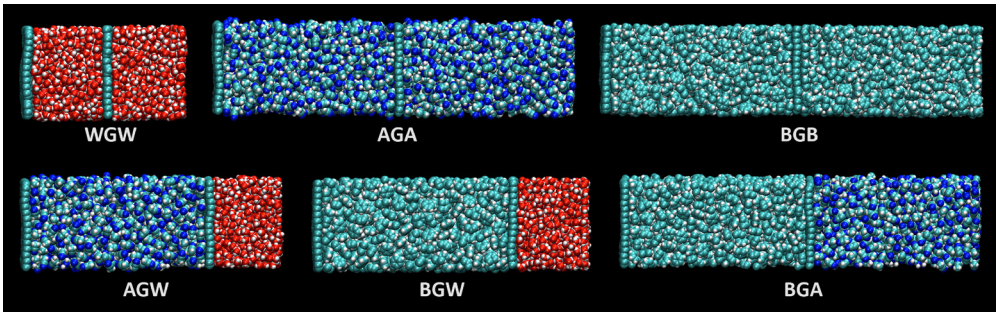

FIG. 1. (Color online) Snapshots of the XGY systems obtained at *NPT* ensembles, with X, Y=W, A, or B. The *z*-direction is perpendicular to the graphene surface. The fluid phases near the graphene membrane remain dense, without any apparent dilution into a low-density hydrophobic interface.

tigated considering large-scale simulations under realistic thermodynamics conditions.

In this paper we give attention to the dynamic, structural, and electrostatic behavior of liquids separated by a single graphene sheet at ambient conditions based on classical MD simulations. We analyze the translational motion and diffusion, density, and electrostatic profiles, as well as the average orientation of the interfacial molecules, for water (a protic and polar medium), acetonitrile (an aprotic and polar medium), and benzene (an aprotic and apolar medium). Thus, we assess the impact of a graphene sheet in the liquid separation involving similar or distinct phases. We investigate how the presence of graphene induces changes in the densities of the two separated liquids, forming an extended interfacial region (including the graphene sheet). By calculating the mass and charge densities of every component as a function of the direction perpendicular to the graphene surface, it is possible to evaluate the interfacial changes for the separated systems. Furthermore, the diffusion properties parallel and perpendicular to the graphene sheet can indicate how the viscosity of these fluids changes as separated by a very thin membrane. In this sense, the present simulations can offer a useful framework to understand structural and thermodynamic properties of interfaces by considering a realistic 2D substrate, instead of defining it as a flat hard wall.[11]

II. MODELS AND METHODS

In our MD simulations we have employed a single graphene sheet (G) to separate two liquid phases (X and Y) forming six distinct XGY systems, where X and Y can be water, acetonitrile or benzene (see Fig. 1). These are given as follows: water-graphene-water (WGW), acetonitrile-graphene-acetonitrile (AGA), benzene-graphene-benzene (BGB), acetonitrile-graphene-water (AGW), benzene-graphene-water (BGW), and benzene-graphene-acetonitrile (BGA). (See Ref. 29.)

For the water–graphene interactions, there are several Lennard–Jones (LJ) potentials developed to reproduce the wetting properties of graphite and carbon nanotubes.[30–34] Thus, we have chosen a useful C–O hydrophobic potential proposed in Ref. 31 for water between graphite plates (see Ref. 29). This choice is also important for future investigation of the present systems in the presence of an electric field. For the acetonitrile molecules, we have used a six-site model[35] that can reproduce in good agreement diverse properties of the liquid (e.g., the experimental density is reproduced within 4%). Similarly, in the case of benzene, an all-atom model developed to describe the aromatic–aromatic interactions of pure liquid benzene and the benzene dimer in solutions[36] was utilized here. It is important to note that the potential models of acetonitrile and benzene contain partial charges, which are very important for the description of the electrostatic profiles and short-range order effects. Thus, the liquid–graphene interactions were modeled by appropriate LJ potentials, whereas the liquid–liquid interactions were calculated by adding the corresponding Coulomb term in the potential function. For our purpose, the interatomic interactions in graphene were taken into account by using harmonic force fields within the OPLS prescription. (See Ref. 29.)

The number of liquid molecules in each one of the XGY systems is given in Ref. 29. We have employed the isobaric-isothermal (*NPT*) ensemble with $P=1$ bar and $T=298$ K to obtain appropriate densities of these systems. In order to compare the ensemble effects we ran a canonic (*NVT*) ensemble for the WGW system by using the equilibrated cell at *NPT* as input. Also, the impact of high pressures (1 to 10 kbar) was investigated for WGW (see Ref. 29). All these systems were equilibrated for at least 1.0 ns and the final configurations were stored after 3.0 ns equilibration processes. The dynamic properties of our systems are properly described by considering the mean square displacement (MSD) (see Ref. 29).

III. RESULTS AND DISCUSSION

Our main concern here is to understand the interfacial properties of polar and nonpolar liquids when they are separated by only a monoatomic carbon layer. Additionally, we are interested in realize how these liquid phases interact with each other through the membrane. A potential experiment could be performed for this purpose with the development of large-area, single layer graphene sheets and with the use of capillary tubes.[1,6,37,38] We note that this could be useful to provide a way of measuring the interfacial width directly from the density profiles of each liquid phase, as well as evaluating the impact of intermolecular interactions between different media separated by a truly 2D membrane. Using different combinations of the liquids, we have obtained diverse wettability patterns of the graphene membrane. Snapshots of each of the systems are displayed in Fig. 1 as obtained from *NPT* ensembles.

TABLE I. Perpendicular ($\perp$) and parallel ($\parallel$) lateral diffusion coefficients (in 10^{-5} cm^2 s^{-1}) for the liquid molecules calculated by using linear fit of the MSD from 0 to 200 ps.

System	$D_L^{\perp}$	$D_L^{\parallel}$
W in (WGW)	4.52 ± 0.20	7.04 ± 0.49
W in (AGW)	6.33 ± 1.68	9.26 ± 2.68
W in (BGW)	4.13 ± 0.51	6.59 ± 0.25
A in (AGA)	3.13 ± 0.38	4.02 ± 0.76
A in (WGA)	2.61 ± 0.97	3.52 ± 0.76
A in (BGA)	2.75 ± 0.05	3.13 ± 0.42
B in (BGB)	1.55 ± 0.19	2.07 ± 0.20
B in (WGB)	1.89 ± 0.24	2.23 ± 0.20
B in (BGA)	2.13 ± 0.01	2.47 ± 0.18

Before examining the dynamic and structural properties of the XGY systems, let us briefly discuss the ensemble effects in the WGW density profile (see Ref. 29). We noted that the oscillations in the density near the graphene surface are much more pronounced at the *NVT* than at the *NPT* ensemble. Also, the variation in the box dimensions at *NPT* allows a greater mobility for the molecules arranging themselves near the surface in comparison with *NVT*. Interfacial layering is clear in the first three water layers of both ensembles, although at *NVT* the density in the first layer increases about three times compared to the bulk density (from 1×10^3 to $\sim 3 \times 10^3$ kg m^{-3}). In the *NPT* case the density of the first layer increases two times compared to the bulk density, going from 1×10^3 to 2×10^3 kg m^{-3}. Additionally, we observed a significant difference in the width of the peak related to graphene, which is wider for the density obtained with the *NPT* simulation. This broadening is mainly associated with the flexibility of the sheet, leading to a relative reduction in the water density near the graphene surface in the *NPT* ensemble. Overall, this analysis shows that the density profile is strongly dependent on the ensemble and that an appropriate description of a more realistic graphene membrane[39,40] separating liquid phases should be obtained at *NPT*.

To examine the translational motion of the molecules along the graphene sheet, we have computed the lateral MSD averaging over the center-of-mass of the molecules in XGY (see Ref. 29). As a sensitive measure of the effect of the local environment of the liquid molecules in the graphene layers, we have also computed the velocity autocorrelation function (VACF) perpendicular to the membrane surface. Thus, we examine the normal displacement effects related to the graphene sheet. Calculated diffusion constants from MSD and VACF are given in Ref. 29. Here, we have considered the motion of the liquid phases perpendicular and parallel to the graphene surface using the MSD. Although the motion at long time maintains the linear diffusive regime, there are appreciable differences in the lateral diffusion calculated for the distinct planes. Recently, a MD simulation study of nanoscale water film on graphene has revealed a fast diffusion of water near the surface.[39] Our calculated lateral diffusion coefficients for the XGY systems are shown in Table I, and we have observed that the parallel diffusion is faster than its perpendicular counterpart. This can be understood through the structuring of the liquids along the z direction, that present free-standing solvation layers. As we shall see later, there are other factors concurring for the behavior of the liquids near the graphene surface.

With respect to the WGW system, we noted a faster diffusion of liquid water when acetonitrile was introduced at the other side of graphene, and a slower diffusion when benzene was considered at the other side. For the three types of liquid, we have observed significant changes in the lateral diffusion coefficients as a function of the liquid placed on the other side of the graphene sheet. Thus, in the case of water we have calculated values of 9.26×10^{-5} cm^2 s^{-1} in AGW and 6.59×10^{-5} cm^2 s^{-1} in BGW for the parallel lateral diffusion constants. These changes can indicate a possible environment effect through the graphene membrane. It is important to note that, when we fix X in the XGY systems and let Y change on the other side of the surface, the systems are kept in the same thermodynamic conditions, with the only difference being their compositions. Thus, the changes in the diffusivity at one side of the box are consequence of the type of liquid at the other.

The liquid structuring and the interactions through the graphene membrane can be realized by a careful investigation of the density profiles displayed in Fig. 2. First, we have analyzed the XGX systems, where strong oscillations were observed for the three systems (WGW, AGA, and BGB). In all these systems the membrane is located in the mid-plane (at $z=0$ nm). The structural behavior of the water molecules along the z axis in WGW reveals that they exhibit bulk properties beyond 1.2 nm from the graphene sheet, leading to a thin interfacial region with thickness of ~ 2.4 nm. It is also interesting to note that the wetting behavior in WGW is opposite of that expected for water near large nonpolar solutes. In the latter case, the water density at contact gradually decreases by increasing the solute size, and the interfacial density profile is broadened by capillary waves.[10] Although the graphene membrane is nonpolar, the extent of water densification in the first hydration layer is comparable to results obtained near polar hydrophilic surfaces.[16] In this sense, a graphene sheet cannot be considered as a hypothetical hydrophobic surface where a water density depletion relative to the bulk is expected near the surface.[18,41] On the contrary, our simulations show that the water density profile near graphene is comparable to that near bare graphite,[20] and is more structured as compared to the density profile of the water–diamond interface.[42]

For the AGA system we can observe structuring effects of acetonitrile up to 1.6 nm, which leads to a wide interfacial region with thickness of ~ 3.2 nm. The largest interfacial region (~ 5 nm) was calculated for BGB, where the structuring exceeds 2.5 nm and five layers are evident. There are previous MD simulations of benzene on graphite[43–45] employing stationary potential walls to represent the graphite substrate. As noted in Ref. 44, benzene is well structured near graphite presenting five peaks in density profile but loosing the short-range order at the temperature around 240 K. In fact, these models are very efficient to reduce the number of nonbonded interactions terms in very large scale simulations; however, they lose important atomic details of the

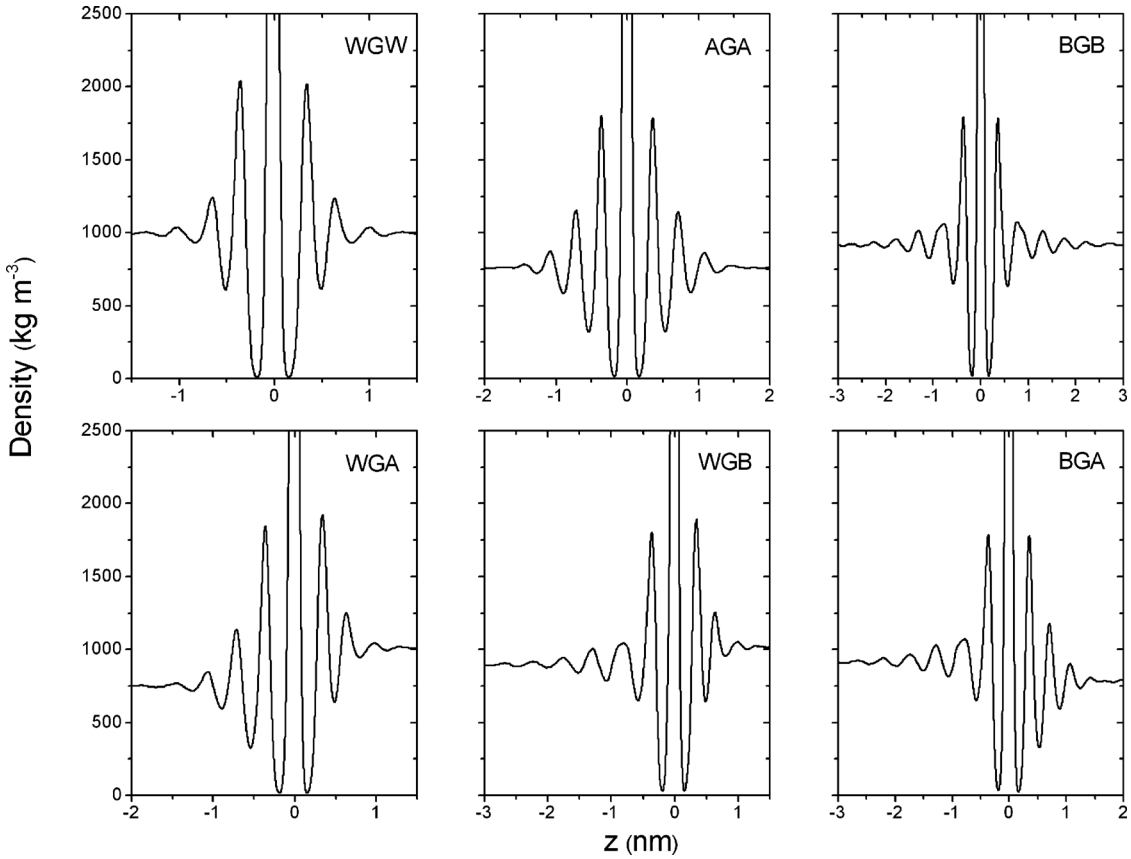

FIG. 2. Mass density distribution computed for the XGY systems under ambient conditions. The density of the fluid phase from the graphene membrane varies considerably along the z direction. In the case of organic liquids the dense region is larger.

surface. In our simulations, we have considered an all-atom model[36] for describing the benzene molecules. In this case, the partial charges on each molecule are important to account for the short-range ordering effects in the liquid, although benzene is a nonpolar liquid. Moreover, the graphene substrate is explicitly included in our dynamics, and its carbon atoms interact via LJ potential with the molecules of the liquid phases. Thus, at ambient conditions, we have obtained very structured patterns near the surface for the BGY systems.

This structural analysis is confirmed by the highly intense peaks observed near graphene in the BGW and BGA systems, as shown in Fig. 2. In the same way, the acetonitrile molecules (described with a six-site model[35]) on the graphene surface are more closely packed. Therefore, benzene and acetonitrile can form long-ranged structured systems when separated by a graphene membrane under ambient conditions. These results can lead to important implications for the crystallization of molecules near a flat solid surface; for example a rapid crystal growing induced by one atom thick membrane. Interestingly, the excluded molecules near graphene lead to packing effects in the closest layers and avoid capillary-wave effects in the liquid–graphene interface.[10] In particular, in the case of WGW, we found that water molecules are excluded from a small region with thickness of ~0.2 nm, with the density rising sharply outside this excluded volume and the first peak extending up to 0.35 nm.

Now, by considering the substitution of water at one side of the WGW box for benzene, to form the BGW system, only small changes are produced in the wetting behavior of the aqueous environment near the graphene surface. A similar pattern is obtained if we include acetonitrile instead of benzene, forming the AGW system (see Ref. 29). As we will discuss later, this is a consequence of the small dispersion interactions of these liquids with water through the membrane. Still considering the density profile, we have obtained slight changes in the heights of the density peaks for the cases of BGW and AGW compared to BGB and AGA, respectively. This effect is, however, more pronounced in the BGA system, forming a very large interfacial region (larger than ~4 nm). It is also worth to mention here that in the case of BGW and BGA, the liquid (water or acetonitrile) in one side of the membrane alters more significantly the wettability of benzene on the other side. We have obtained an increment of ~100 kg/m^3 in the first layer of benzene by changing water for acetonitrile on the other side. Also, comparing AGW and BGA, we noted that benzene and water influence differently the wettability of acetonitrile.

As important as the mass density profile, the charge density distribution of the separated liquids indicates the orientation tendencies for the media near the membrane. In Fig. 3, we plot the charge density distribution of the XGY systems along the z-coordinate. All these systems exhibit positive peaks near the graphene surface, indicating the presence of some interfacial hydrogen atoms. This is particularly inter-

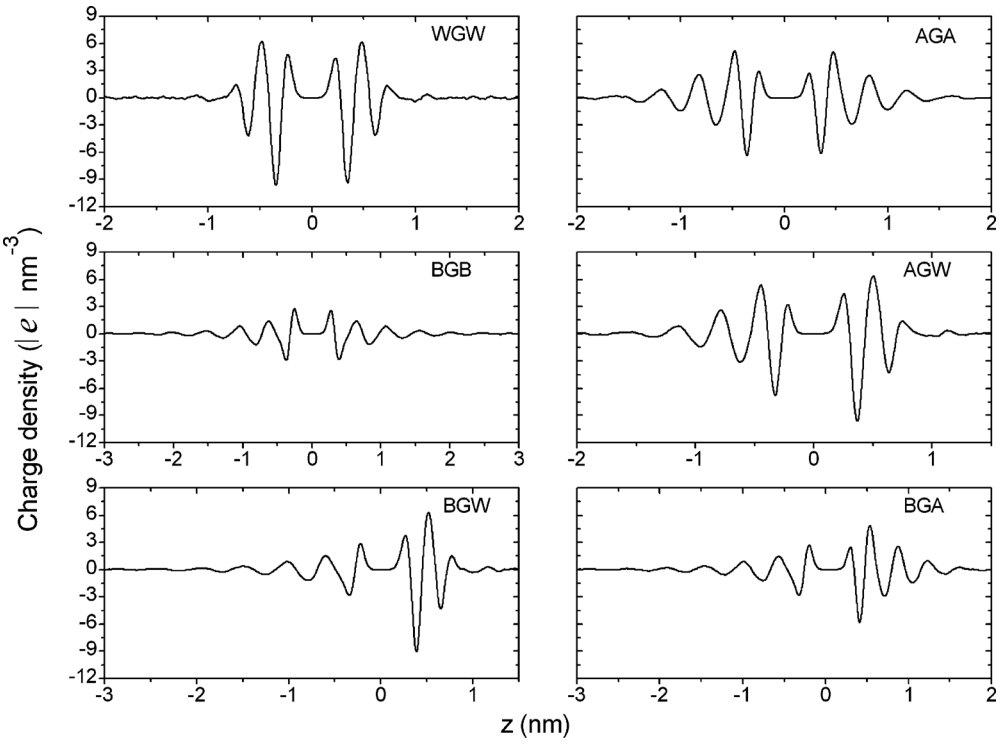

FIG. 3. Charge density distribution computed for the XGY systems under ambient conditions. In all these systems we have employed appropriate charged potential models.

esting in the case of the BGY systems, where the benzene molecules show a preference to be bent with respect the surface. As expected for high temperatures, the interfacial benzene molecules present an angular distribution[44] with the orientation of the molecules less flat to the surface. This is evident when we analyze the atomic charges profile of benzene in the direction perpendicular to the graphene surface. We have obtained the first peak of BGB starting at +3 $|e|/\mathrm{nm}^3$ around 0.27 nm to the surface. The intensity of the second peak is reduced to half at 0.65 nm and third peak is only +0.8 $|e|/\mathrm{nm}^3$ at 1 nm from the surface. Beyond this range we noted more two small peaks extending up to 2 nm, indicating a loss of structuring of the benzene molecules in the bulk.

In all the XGY systems the highest peaks were observed in the XGW systems. For WGW, we noted the first peak (with +4.6 $|e|/\mathrm{nm}^3$ at 0.27 nm) in the region from which water molecules are excluded, which decreases sharply to around -9 $|e|/\mathrm{nm}^3$ at 0.37 nm from the surface. These findings are consistent with the preference for some interfacial water molecules to be oriented with an OH bond pointing toward the graphene surface.[28] Also, *ab initio* calculations have indicated that orientations with one OH bond parallel and the other one pointing to the graphene surface are energetically more favorable.[46] A similar feature was noted when we analyzed the AGW box, with the first peak slightly reduced to approximately +4 $|e|/\mathrm{nm}^3$ in BGW. On the other hand, in the case of acetonitrile we noted an appreciable interphase effect on the distribution of the acetonitrile charge density. For example, in AGW the first peak is less intense (+3.4 $|e|/\mathrm{nm}^3$) than in BGA (+2.7 $|e|/\mathrm{nm}^3$), which indicates a stronger influence of benzene than water on the other side of the membrane. In fact, in our approach these effects are described only considering an average influence of graphene, provided by the dispersion interactions. In a more realistic model, possible screening effects could affect the interactions between fluids separated by the graphene sheet.

A deeper analysis of the average orientation of the interfacial molecules was also performed by calculating their angular distribution as shown in Fig. 4. In the cases of water and acetonitrile, we have used the angle (θ) between the molecular dipole moment and the graphene surface normal, whereas for benzene this angle was calculated with respect to the aromatic ring normal. Here it is important to note that the surface normal vector is defined as pointing toward each liq-

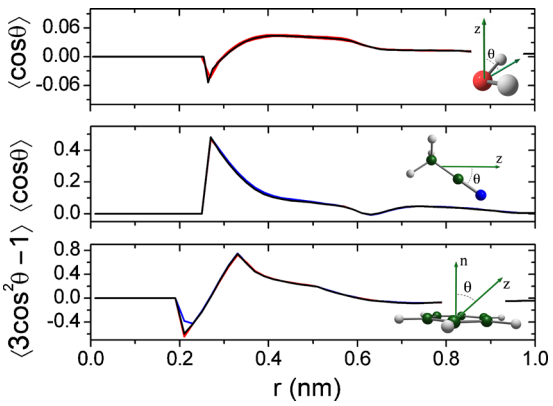

FIG. 4. (Color online) Orientational distribution of the molecules with respect to the surface normal of the graphene sheet. The average orientations of water, acetonitrile, and benzene are shown on the top, middle, and bottom panels, respectively. For the polar systems the mean of cos θ was calculated, whereas for benzene the mean of ($3\cos^2\theta - 1$) was calculated.

TABLE II. Interaction energies (in kJ mol^{-1}) between the liquid and graphene (XG or GY) and liquid-liquid through graphene (XY) for the XGY.

System	XG	GY	XY
WGW	−1643 ± 48	−1643 ± 48	−39.1 ± 2.4
AGA	−2459 ± 56	−2459 ± 56	−100.5 ± 2.7
BGB	−2520 ± 52	−2520 ± 52	−110.5 ± 3.0
AGW	−2435 ± 41	−1666 ± 34	−65.9 ± 2.3
BGW	−2480 ± 42	−1698 ± 34	−66.5 ± 2.3
BGA	−2496 ± 41	−2498 ± 41	−105.4 ± 3.1

uid phase. Thus, the mean value of the cos θ was calculated for water and acetonitrile and the mean value of $(3\cos^2\theta - 1)$ was calculated for benzene.

As displayed on the top panel, the water molecules do not exhibit a well organized distribution near the surface under ambient conditions. We have only observed a small peak at 0.25 nm in the XGW systems. On the middle panel we show the orientation of the acetonitrile molecules in the different systems. In this case, we noted that the average dipole moments are distributed around 66° in the first layer near graphene. This is also consistent with our analysis of the charge distribution profiles for acetonitrile (Fig. 2). Finally, for the benzene molecules, the orientational distribution in the BGY systems indicate that some molecules are forming an angle around 63° with respect to the surface. As we have mentioned before, flat configurations of benzene molecules are not expected under ambient conditions. Also, as observed recently[47] adsorbed benzene on the silica surface reveal a strong layering that decays with the distance from the substrate.

The structural and electrostatic analyses presented here are in line with the calculated interaction energies of the liquid with graphene. In Table II, we give the calculated interaction energies of all these liquid phases with the graphene surface and between them. As can be seen, the water–graphene interaction slightly decreases in the following order: BGW (−1698 kJ/mol), AGW (−1666 kJ/mol), and WGW (−1643 kJ/mol). On the other hand, the benzene–graphene interaction is −2520 kJ/mol in BGB, −2496 kJ/mol in BGA and −2480 kJ/mol in BGW. In the case of acetonitrile, its interaction with graphene decreases in the order BGA to AGA to AGW. Indeed, we noted that the liquid–graphene interaction for a reference liquid always increases in the same order: W < A < B in all these systems. More interestingly, the same trends are noted comparing the liquid–liquid interactions through the membrane (see Table II).

This analysis is consistent with our atomistic models and physically acceptable since the dispersion interactions are expected to be increasing from water to benzene. Moreover, these findings reinforce the proposal that a liquid at one side of the graphene surface can directly influence the structural properties of another liquid in the other side. Also, these interphase effects seems to be in agreement with recent *ab initio* calculations[9] for water adsorption in suspended graphene. Thus, we expect that some properties can be significantly modified by simply interchanging the graphene-separated liquid phase. In particular, future implementations for the interfacial excess free energy calculations[48] of these solid–liquid interfaces could be useful to elucidate the thermodynamics of the interfacial region, which consists of a single graphene sheet surrounded by liquids with different polarities.

IV. CONCLUDING REMARKS

We have reported a computational analysis of the dynamic, structural, and electrostatic properties of liquids with different polarities, separated by a graphene membrane. These properties have been obtained via extensive classical MD simulations. The reliability of our results is supported by the use of appropriate atomistic potential models for the liquid–liquid and liquid–graphene interactions. Moreover, we have employed a proper ensemble (*NPT*) containing thousands of molecules, and including explicitly the dynamics of the graphene sheet, which might be essential for producing accurate results for the studied systems. We have focused on the structures of water, acetonitrile, and benzene when they are separated by a single graphene sheet at ambient conditions. Our simulations consistently showed strong density oscillations and an asymmetric wetting behavior for different combinations of liquids near the separation surface. We found that the interfacial behavior can be induced by interactions of the liquids with the carbon atoms, as well as with the liquid placed on the other side of the membrane.

In the case of the aqueous system, the structuring of water near the graphene surface is extremely local, forming a thin interfacial region under atmospheric pressure but extending to larger regions under high pressures. Also, the microscopic structure of the water layers in WGW was less altered by changing the type of liquid at one of the sides of the box. In the case of benzene and acetonitrile, the interfacial densification is broadened by very strong dispersion forces with graphene. Different from the water behavior, the organic liquids appear to be more sensitive to the type of liquid placed at the other side of the membrane. This study have pointed out that it is possible to realize the microscopic structure of different liquids separated by a graphene membrane. For example, we noted that the liquid–graphene interaction for a reference liquid at one side of the XGY box increases in the order W < A < B in all these systems. Additionally, we expect that, with the rapid advances in the synthesis of macroscopic graphene membrane, this study can be useful to understand interfacial problems of liquids separated by a truly 2D membrane at ambient conditions.

ACKNOWLEDGMENTS

This work was partially supported by the Brazilian agencies: CNPq, FAPESP, and FAPESB. The authors thank Dr. Luciano T. Costa for his kind interest and important suggestions for the computational calculations.

[1]T. J. Booth, P. Blake, R. R. Nair, D. Jiang, E. W. Hill, U. Bangert, A. Bleloch, M. Gass, K. S. Novoselov, M. I. Katsnelson, and A. K. Geim, Nano Lett. **8**, 2442 (2008).
[2]A. K. Geim, Science **324**, 1530 (2009).
[3]J. S. Bunch, S. S. Verbridge, J. S. Alden, A. M. van der Zande, J. M.

Parpia, H. G. Craighead, and P. L. McEuen, Nano Lett. **8**, 2458 (2008).
[4]N. Inui, K. Mochiji, and K. Moritani, Nanotechnology **19**, 505501 (2008).
[5]R. B. Pontes, A. Fazzio, and G. M. Dalpian, Phys. Rev. B **79**, 033412 (2009).
[6]A. A. Green and M. C. Hersam, Nano Lett. **9**, 4031 (2009).
[7]C. E. Hamilton, G. R. Lomeda, Z. Sun, J. M. Tour, and A. R. Barron, Nano Lett. **9**, 3460 (2009).
[8]M. D. Lacasse, G. S. Grest, and A. J. Levine, Phys. Rev. Lett. **80**, 309 (1998).
[9]T. O. Wehling, A. I. Lichtenstein, and M. I. Katsnelson, Appl. Phys. Lett. **93**, 202110 (2008).
[10]J. Mittal and G. Hummer, Proc. Natl. Acad. Sci. U.S.A. **105**, 20139 (2008).
[11]H. S. Ashbaugh and L. R. Pratt, Rev. Mod. Phys. **78**, 159 (2006).
[12]S. Esteban-Martín, H. J. Risselada, J. Salgado, and S. J. J. Marrink, J. Am. Chem. Soc. **131**, 15194 (2009).
[13]J. Wong-Ekkabut, S. Baoukina, W. Triampo, I. Tang, D. P. Tieleman, and L. Monticelli, Nat. Nanotechnol. **3**, 363 (2008).
[14]M. L. Berkowitz, D. L. Bostick, and S. Pandit, Chem. Rev. **106**, 1527 (2006).
[15]N. Shenogina, R. Godawat, P. Keblinski, and S. Garde, Phys. Rev. Lett. **102**, 156101 (2009).
[16]R. Notman and T. R. Walsh, Langmuir **25**, 1638 (2009).
[17]L. Hua, Z. Zangi, and B. J. Berne, J. Phys. Chem. C **113**, 5244 (2009).
[18]R. Vácha, Z. Zangi, J. B. F. N. Engberts, and P. Jungwirth, J. Phys. Chem. C **112**, 7689 (2008).
[19]P. Hirunsit and P. B. Balbuena, J. Phys. Chem. C **111**, 1709 (2007).
[20]D. Bedrov and G. D. Smith, Langmuir **22**, 6189 (2006).
[21]L. Lu and M. L. Berkowitz, J. Chem. Phys. **124**, 101101 (2006).
[22]R. Zangi and J. B. F. N. Engberts, J. Am. Chem. Soc. **127**, 2272 (2005).
[23]N. Choudhury and B. M. Pettitt, J. Phys. Chem. B **109**, 6422 (2005).
[24]N. Choudhury and B. M. Pettitt, J. Am. Chem. Soc. **127**, 3556 (2005).
[25]A. Striolo, A. A. Chialvo, P. T. Cummings, and K. E. Gubbins, Langmuir **19**, 8583 (2003).
[26]L. Itzhaki, E. Altus, H. Basch, and S. Hoz, J. Phys. Chem. C **112**, 1925 (2008).
[27]A. A. Chialvo and J. M. Simonson, J. Phys. Chem. C **112**, 19521 (2008).
[28]G. Cicero, J. C. Grossman, E. Schwegler, F. Gygi, and G. Galli, J. Am. Chem. Soc. **130**, 1871 (2008).
[29]See supplementary material at http://dx.doi.org/10.1063/1.3518507 for details of the models, for LJ parameters in Table S1, atomistic parameters and comparisons of mass and electrostatic density distributions simulated with all-atom and united-atom sites are provided in the SI, Figure S5 in the SI, Figure S3 in the SI, and Figure S6 in the SI.
[30]T. Werder, J. H. Walther, R. L. Jaffe, T. Halicioglu, and P. Koumoutsakos, J. Phys. Chem. B **107**, 1345 (2003).
[31]S. Vaitheeswaran, H. Yin, and J. C. Rasaiah, J. Phys. Chem. B **109**, 6629 (2005).
[32]M. C. Gordillo and J. Martí, Phys. Rev. B **78**, 075432 (2008).
[33]S. Joseph and N. R. Aluru, Nano Lett. **8**, 452 (2008).
[34]A. Striolo, A. A. Chialvo, P. T. Cummings, and K. E. Gubbins, J. Chem. Phys. **124**, 074710 (2006).
[35]X. Grabuleda, C. Jaime, and P. A. Kollman, J. Comput. Chem. **21**, 901 (2000).
[36]W. L. Jorgensen and D. L. Severance, J. Am. Chem. Soc. **112**, 4768 (1990).
[37]X. Li, Y. Zhu, W. Cai, M. Borysiak, B. Han, D. Chen, R. D. Piner, L. Colombo, and R. S. Ruoff, Nano Lett. **9**, 4359 (2009).
[38]E. Stolyarova, D. Stolyarov, K. Bolotin, S. Ryu, L. Liu, K. T. Rim, M. Klima, M. Hybertsen, I. Pogorelsky, I. Pavlishin, K. Kusche, J. Hone, P. Kim, H. L. Stormer, V. Yakimenko, and G. Flynn, Nano Lett. **9**, 332 (2009).
[39]J. H. Park and J. Aluru, PhysChemComm **114**, 2595 (2010).
[40]A. Fasolino, J. H. Los, and M. I. Katsnelson, Nature Mater. **6**, 858 (2007).
[41]D. A. Doshi, E. B. Watkins, J. N. Israelachvili, and J. Majewski, Proc. Natl. Acad. Sci. U.S.A. **102**, 9458 (2005).
[42]F. Sedlmeier, J. Janecek, C. Sendner, L. Bocquet, R. R. Netz, and D. Horinek, Biointerphases **3**, FC23 (2008).
[43]R. G. Winkler and R. Hentschke, J. Chem. Phys. **100**, 3930 (1994).
[44]M. A. Matties and R. Hentschke, Langmuir **12**, 2495 (1996).
[45]B. Clifton and T. Cosgrove, Mol. Phys. **93**, 767 (1998).
[46]O. Leenaerts, B. Partoens, and F. M. Peeters, Phys. Rev. B **77**, 125416 (2008).
[47]B. Coasne, C. Alba-Simionesco, F. Audonnet, G. Dosseh, and K. E. Gubbins, Langmuir **25**, 10648 (2009).
[48]F. Leroy, F. J. V. A. dos Santos, and F. Müller-Plathe, Macromol. Rapid Commun. **30**, 864 (2009).